NJC

RSC Publishing

PAPER

View Article Online
View Journal | View Issue

Cite this: *New J. Chem.*, 2013, **37**, 992

Redox-active proligands from the direct connection of 1,3-dithiol-2-one to tetrathiafulvalene (TTF): syntheses, characterizations and metal complexation†

Franck Camerel,* Olivier Jeannin, Gilles Yzambart, Bruno Fabre, Dominique Lorcy and Marc Fourmigué

Received (in Montpellier, France) 3rd December 2012, Accepted 11th January 2013

DOI: 10.1039/c3nj41097h

www.rsc.org/njc

In the search for novel tetrathiafulvalene-substituted dithiolene ligands, two tetrathiafulvalene (TTF) molecules directly connected to 1,3-dithiol-2-one fragments have been synthesized and characterized by single crystal X-ray diffraction, electrochemical and spectroscopic analyses. **TTF1** was obtained, in moderate yield, by the cross-coupling of 4,5-bis(methylthio)-1,3-dithiole-2-one with 4,4′-bis(1,3-dithiole-2-one) in triethylphosphite, whereas for **TTF2**, the 1,3-dithiol-2-one fragment was introduced, in high yield, by an original reaction of the alkyne group of an ethynyl TTF (Me_3TTF–C≡CH) with xanthogen in the presence of a radical initiator. Opening of the 1,3-dithiol-2-one fragments with sodium methanolate leads to the formation of two new 1,2-dithiolate ligands functionalized with redox-active TTF moieties, which can efficiently coordinate metals. As an illustration, two original heteroleptic bis(cyclopentadienyl)dithiolene titanium complexes were isolated and characterized.

Introduction

New tetrathiafulvalene (TTF) derivatives continue to be of great importance for the study of crystalline charge transfer and radical ion salts which are relevant for the synthesis of organic molecular conductors and magnetic materials.[1] The redox properties of the tetrathiafulvalene (TTF), associated with its strong π-electron donor ability, have also attracted a lot of attention in the preparation of molecular systems in which the electronic properties of the molecule in solution can be controlled with the oxidation state of the TTF moieties.[2] Especially, numerous metal complexes with TTF containing ligands have been engineered to display a wide range of attractive applications, such as sensors, receptors and switches.[3] For this purpose, various coordination functions, such as pyridine, polypyridine, phosphine, acetylacetonate and so on, have been grafted on the TTF core in order to convert the TTF into an electroactive ligand for the elaboration of hybrid multifunctional materials.[4] Amongst all these examples, the TTF-dithiolates are particularly interesting, especially because after metal complexation to form metal–dithiolene complexes, they give rise to single component molecular metals with 3-D conductivity. For example, Kobayashi *et al.* have reported that crystals of the neutral [Ni(tm-TTFdt)$_2$] metal–bis(dithiolene) complexes carrying two TTF fragments showed a room temperature conductivity of 400 S cm^{-1} and metallic behaviour down to 0.6 K.[5] Also, TTF-dithiolate–metallocene complexes can lead after one-electron oxidation to molecular materials with high electrical

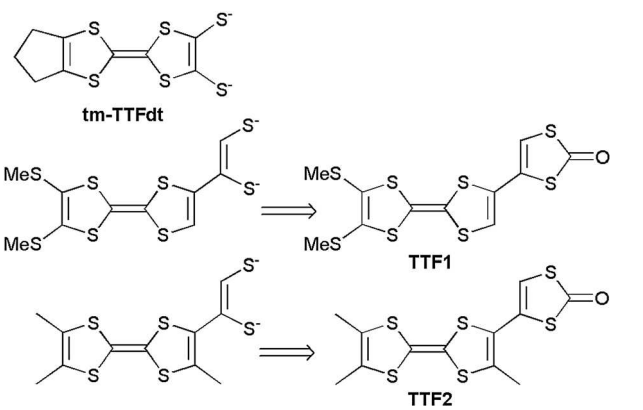

Chart 1 Chemical structures of tm-TTFdt and the targeted molecules **TTF1** and **TTF2**.

Institut des Sciences Chimiques de Rennes, UMR 6226 CNRS-Université de Rennes 1, Matière Condensée et Systèmes Electroactifs (MaCSE), Campus de Beaulieu, 35042 Rennes, France. E-mail: franck.camerel@univ-rennes1.fr

† Electronic supplementary information (ESI) available: UV-vis absorption spectra of TTF derivatives. CCDC 913393, 913394, 913395, and 913396 for **TTF1**, **TMT-bi-TTF**, **TTF2** and by-product respectively. For ESI and crystallographic data in CIF or other electronic format see DOI: 10.1039/c3nj41097h

conductivities.[6] In order to develop this attractive family of compounds, we have undertaken the exploration of novel TTF derivatives functionalized by non-fused dithiolene moieties, as illustrated in Chart 1, which could give access to a wide variety of metal complexes with multiple redox systems.[7]

Such dithiolate ligands should be easily generated from the corresponding 1,3-dithiole-2-one heterocycles, when reacted with strong nucleophiles.[8] We describe here two synthetic routes toward the TTF-substituted 1,3-dithiole-2-ones **TTF1** and **TTF2**. We also demonstrate that the dithiolone fragment can be indeed opened with a base to obtain the corresponding TTF-dithiolate ligands and that these ligands can efficiently complex a metal centre, such as titanium, to form stable cyclopentadienyl–dithiolene complexes.[9]

Results and discussion

TTF rings connected to 1,3-dithiol-2-one fragments by a single bond have already been described. They can be obtained from the phosphite-mediated cross-coupling method between the 4,4′-bis(1,3-dithiole-2-one) compound and 1,3-dithiole-2-one derivatives,[10] affording the corresponding butylthio and hexylthio derivatives in 31–37% yield. In the present work, we have first explored this route with the 4,5-bis(methylthio)-1,3-dithiole-2-one as starting material. The limitations of this synthetic path will lead us to propose an alternative route, based on the recent availability of TTF alkynyl derivatives (see below).

Synthesis and structure of TTF1

Reaction of 4,4′-bis(1,3-dithiole-2-one) and 4,5-bis(methylthio)-1,3-dithiole-2-one in 1 : 1 ratio in pure triethylphosphite for 1 hour at 110 °C leads to the formation of the targeted **TTF1** in 13% yield. **TTF1** can be isolated in higher yield (31%) by using an excess (1.5 eq.) of 4,4′-bis(1,3-dithiole-2-one), together with the bis-coupled the 4,5,4‴,5‴-tetrakis(methylthio)-4′,4″-bitetrathiafulvalene (**TMT-bi-TTF**) compound in 13% yield (Scheme 1). The yield of **TTF1** decreased for longer reaction times and this is likely attributed to the formation of poorly soluble TTF trimers and higher order oligomers. The molecular structure and purity of the isolated compound after column chromatography were assigned by ^{1}H and ^{13}C NMR spectroscopy, infrared spectroscopy, mass spectrometry and elemental analysis. It should be noted that the **TMT-bi-TTF** compound has already been synthesized by Ullmann coupling from iodo-TTF precursors[11] or transition-metal-catalyzed coupling reactions.[12]

Single crystals of **TTF1** suitable for X-ray analysis were grown by slow evaporation from 1 : 1 CH_2Cl_2 : MeOH solution. The X-ray structures obtained confirm the molecular structure of both compounds. **TTF1** crystallises in the triclinic system, space group $P\bar{1}$, with two crystallographically independent molecules, both in the general position (Fig. 1). For both molecules, the 1,3-dithiole-2-one and the TTF core are coplanar, except for the methyl groups which point out on the same side of the plane. The carbonyl group is oriented parallel to the long axis of the TTF fragment. The central C=C bond lengths (C6–C7 = 1.346(6) and C17–C18 = 1.348(5) Å) in the two TTF cores confirm

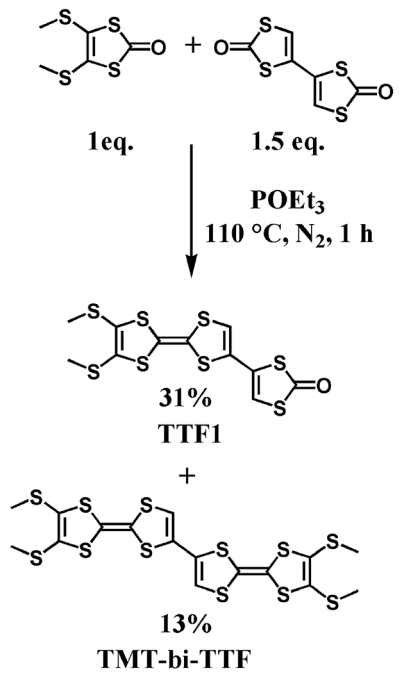

Scheme 1 Synthetic route for the preparation of **TTF1** from 4,4′-bis(1,3-dithiole-2-one) and 4,5-bis(methylthio)-1,3-dithiole-2-one.

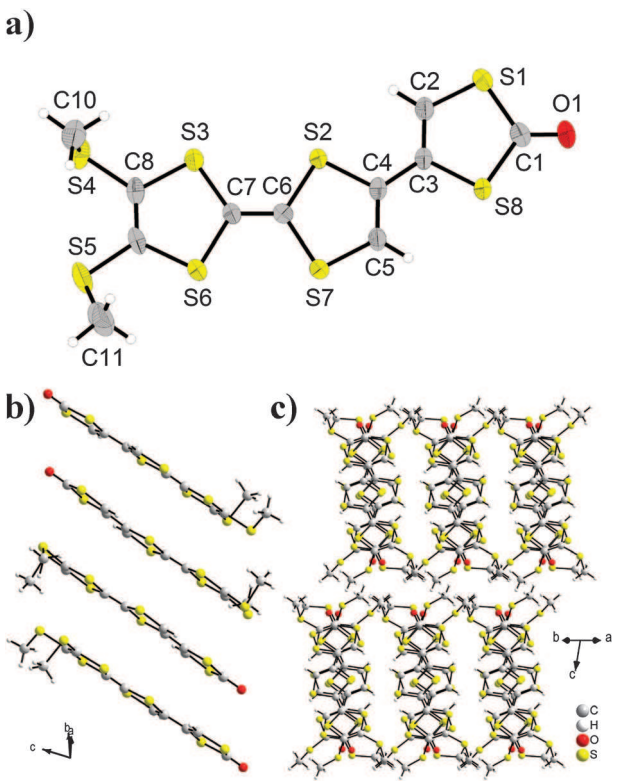

Fig. 1 (a) Molecular structure of the two crystallographically independent **TTF1** molecules with the atomic numbering (ellipsoids drawn at the 50% probability level); (b) representation of the stacks observed along the [110] direction; (c) projection of the crystalline structure along the [110] direction.

that they are in the neutral state (C=C ~ 1.38 Å in the oxidized form). The two crystallographically independent molecules are

associated in the crystal structure into non-centrosymmetrical dimers in which the dithiolone fragments and the TTF cores stack on top of each other, respectively, and all methyl groups point toward the same direction (Fig. 1b). The TTF cores are slightly staggered and the shortest S···S contact is 3.70 Å. These dimers pile up in a head to tail fashion to form stacks running along the [110] direction (Fig. 1b and c).

The crystalline structure of the **TMT-bi-TTF** compound solved in the monoclinic space group $P2_1/n$ has already been described with crystals obtained from CS_2 solutions.[12] This compound shows polymorphism since crystals obtained from CH_2Cl_2 : MeOH solutions crystallize in the orthorhombic system, space group $Pn2_1a$, with one molecule in the general position. The conjugated system containing the two TTF cores is completely flat and only the methyl groups point out of the plane (Fig. 2a). The central C=C bond lengths (C3–C4 = 1.357(10) and C11–C12 = 1.338(10) Å) in both TTF moieties confirm that they are in the neutral state. In the molecular structure, the molecules pile up along the *c* axis to form stacks (Fig. 2b). The molecules are tilted and three-quarter of the molecule overlaps ring over ring the neighbouring molecule (Fig. 2c). The shortest S–S contacts are in the range of 3.70–3.82 Å.

Despite its convenience, this phosphite-mediated coupling reaction's yield hardly exceeds 30%. For this reason, we have also investigated a radical synthetic route, described by Gareau and Beauchemin,[13] where an alkyne derivative R–C≡C–H is reacted with diisopropylxanthogen disulfide to lead, in one step, to the R-substituted 1,3-dithiol-2-one derivatives. This synthetic path has been recently successfully used with ethynyl-indole-derivatives to convert them into the corresponding indole-substituted 1,3-dithiole-2-one derivatives. Base opening and metal complexation afforded original metal–bis(dithiolene) complexes carrying electropolymerisable indole fragments.[14] Its possible application to the preparation of desired TTF derivative **TTF1** or **TTF2** relies therefore on the availability of the corresponding TTF alkyne derivatives.[15] We have recently reported that the trimethyl-TTF derivative Me_3TTF–C≡C–H could be prepared in good yield as a relatively stable compound,[16] for further incorporation on organometallic complexes,[17–19] or for surface modifications.[20]

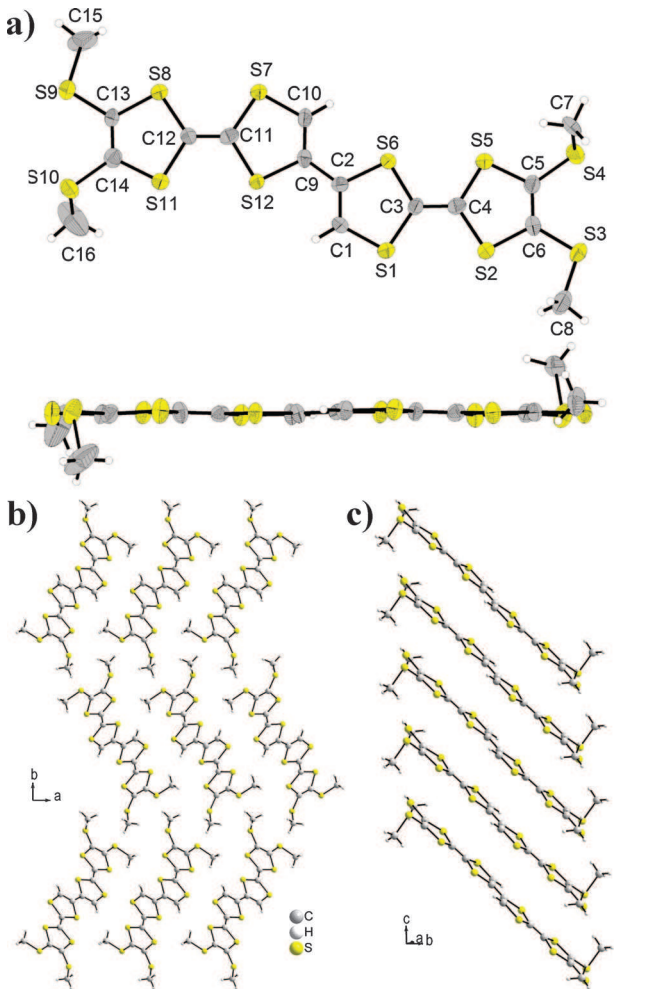

Fig. 2 (a) Molecular structure of the **TMT-bi-TTF** compound with the atomic numbering (top) and side view (bottom) (ellipsoids drawn at the 50% probability level); (b) projection of the crystalline structure along *c*; (c) view of the stacks running along *c*.

Synthesis and structure of TTF2

Accordingly, trimethyl-TTF acetylene was reacted with diisopropylxanthogen disulfide in benzene in the presence of AIBN as a radical initiator (Scheme 2). The targeted **TTF2** was obtained in 60% yield. The molecular structure of **TTF2** was unambiguously confirmed by NMR spectroscopy, mass spectrometry and elemental analysis, as well as X-ray crystal structure analysis. **TTF2** crystallizes in the monoclinic $C2/c$ space group with one molecule per unit cell in the general position. Unlike **TTF1**, the **TTF2** molecule is not planar and the dithiolone fragment is significantly twisted as its mean plane makes a dihedral angle of 38.50° with the aromatic TTF core (Fig. 3a). This deformation is likely induced by the steric constraints imposed by the presence of the methyl group *ortho* to the dithiolone fragment. The rotation of the methyl groups at 293 K introduces some

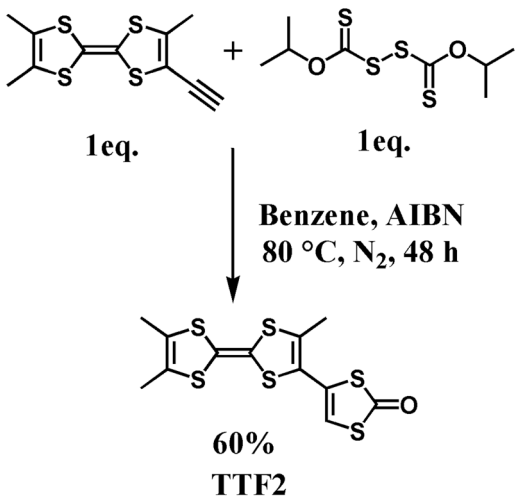

Scheme 2 Synthetic route for the preparation of **TTF2** from ethynyltrimethyl-TTF.

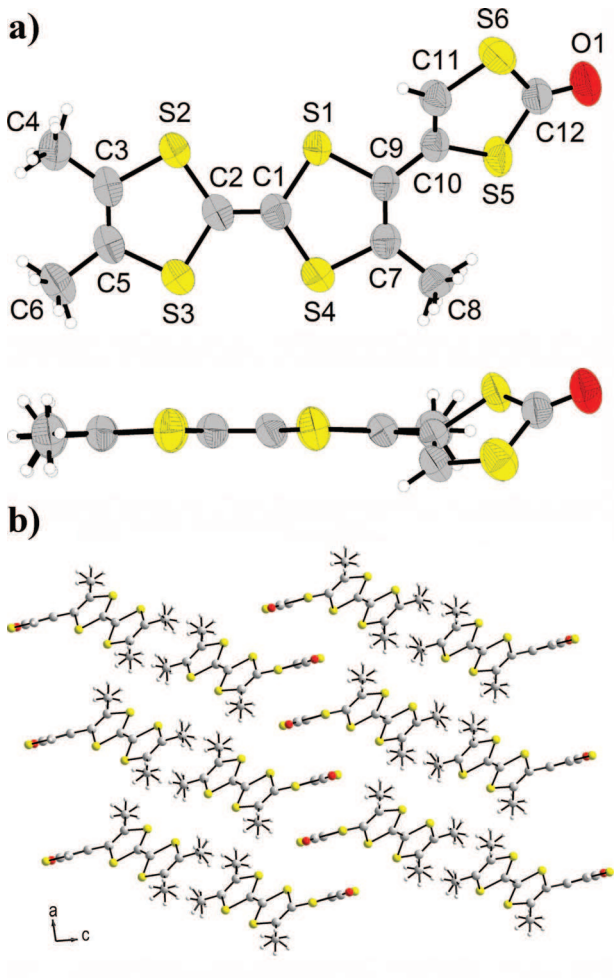

Fig. 3 (a) Molecular structure of **TTF2** with the atomic numbering (top) and side view (bottom) (ellipsoids drawn at the 50% probability level); (b) projection of the crystalline structure along *b*.

disorder. The central C1═C2 distance [1.340(4) Å] in the TTF core confirms its neutral state. The packing of **TTF2** is also different from the one observed with **TTF1**. Projection of the crystalline structure along the *b* axis reveals a clear segregation between the dithiolone fragments and the TTF cores into layers parallel to the (*ab*) plane (Fig. 3b). The molecules are arranged along the *b* axis into highly staggered stacks with almost no overlapping.

During the purification of **TTF2**, an orange-coloured by-product was also easily isolated in 27% yield. The NMR spectrum of this by-product appears to be relatively complicated with the presence of numerous peaks corresponding to methyl groups as well as isopropyl fragments. Single crystals of this by-product, suitable for X-ray analysis, were grown by slow evaporation from 1 : 1 CH_2Cl_2 : MeOH solution and allowed unambiguous determination of the molecular structure of this original compound. The isolated molecule, presented in Fig. 4, contains one TTF molecule, half of one TTF fragment, one thiophene fragment and two xanthate moieties. The formation of this unexpected by-product could be explained by the reaction between two trimethyl-TTF acetylene

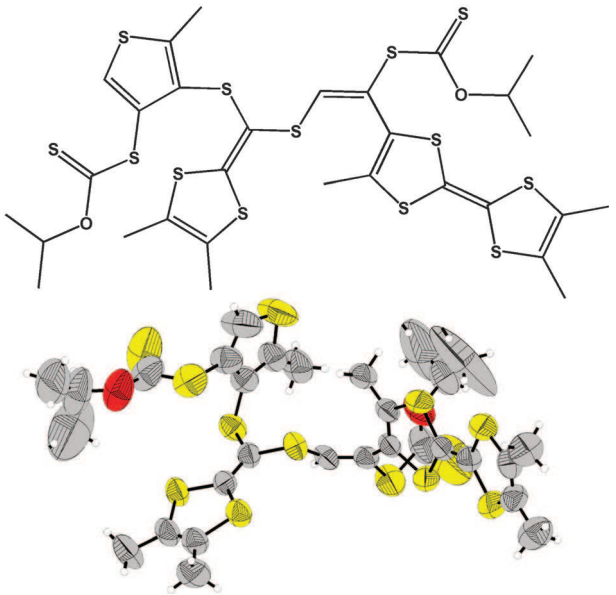

Fig. 4 Molecular structure of the by-product isolated after reaction of ethynyl-trimethyl-TTF with diisopropylxanthogen disulfide (ellipsoids drawn at the 50% probability level).

molecules in which the ethyne groups have been activated by xanthate radicals. One of these activated alkynes reacts directly on the sulfur atom of the second activated ethynyltrimethyl-TTF molecule to open the dithiole ring. The formation of the thiophene fragment likely arises from the trapping of the two free radicals on a sulfur atom available in the reaction mixture.

Spectroscopic and electrochemical properties

The electronic properties of **TTF1** and the newly synthesized **TTF2** derivative were investigated by UV-visible absorption spectroscopy in dichloromethane solutions and by cyclic voltammetry (CV) in CH_2Cl_2 using $[NBu_4][PF_6]$ as the supporting electrolyte. UV-visible and electrochemical data are gathered in Table 1. The spectroscopic and electrochemical properties of the parent $Me_3TTF–C{\equiv}CH$ have also been included for comparison. **TTF2** with methyl substituents shows three main absorption bands centred at 294, 334 and 394 nm which are attributed to $^1\pi$–π^* transitions localized on the TTF core (Fig. 5 and Fig. S1 in ESI†). The CV of **TTF2** displays two perfectly reversible one-electron systems at $E_1^{o'} = 0.44$ V and $E_2^{o'} = 0.91$ V *vs.* SCE (average of the anodic and cathodic peak potentials E_{pa} and E_{pc}) attributed to the formation of the TTF radical cation and dication, respectively. The introduction of the 1,3-dithiole-2-one fragment in place of the alkyne arm weakly affects the electronic properties of the TTF cores as the first oxidation process is anodically shifted by 0.05 V. Substitution of three methyl substituents by two methylthio substituents in **TTF1** induces also an anodic shift of the first oxidation potentials by ~0.01 V, when compared to **TTF2**. The precipitation of the dicationic species on the platinum electrode can be prevented at scanning rates higher than 20 V s^{-1}. Except for a slight increase in the extinction coefficient, the absorption spectrum of **TTF1** is similar to that of **TTF2**.

Table 1 UV-visible[a] and electrochemical data[b] for all compounds

Compound	λ_{max}/nm ($\varepsilon/10^3$ M^{-1} cm^{-1})	$E^{o'}_{ox}$/V *vs.* SCE[c] (ΔE_p/mV)	$E^{o'}_{red}$/V *vs.* SCE[d] (ΔE_p/mV)
$Me_3TTFC{\equiv}CH$	295 (15); 331 (14); 386 (3.0)	0.38; 0.88	
TTF1	300 (20.5); 328 (16); 410 (4.3)	0.53 (70); 0.90 (64)	
TMT-bi-TTF	263 (22); 314 (24); 327 (24); 406 (7.4)	0.49 (64); 0.63 (58); 0.87 (58); 0.95[e]	
TTF2	294 (17.5); 334 (13); 394 (2.5)	0.44 (55); 0.91 (60)	
By-product	292 (36.5); 334 (27); 365 (14); 472 (1.0)	0.32 (70); 0.83 (100); 1.18 (90)	
$(Cp)_2TiCl_2$	255 (23); 314 (5.4); 392 (2.3)		−0.72 (75)
$(Cp)_2$Ti(TTF1)	298 (18.3); 312 (18.7); 329 (17.7); 415 (6.0); 673 (2.4)	0.40 (60); 0.84 (80)	−1.00 (82)
$(Cp)_2$Ti(TTF2)	307 (18); 332 (15); 430 (3.7); 680 (1.9)	0.24 (76); 0.72 (88)	−1.05 (88)

[a] Electronic absorption data measured in CH_2Cl_2 at room temperature ($c \sim 10^{-5}$ mol L^{-1}). [b] In CH_2Cl_2–NBu_4PF_6 0.2 M at room temperature; scan rate: 0.1 V s^{-1}. [c] Formal potentials corresponding to different reversible oxidation processes, taken as the middle of the anodic and the cathodic peak potentials; ΔE_p: peak-to-peak separation. [d] Formal potential corresponding to the reversible reduction of Ti^{4+} to Ti^{3+}. [e] Anodic peak potential due to the adsorption of the charged species on the electrode surface.

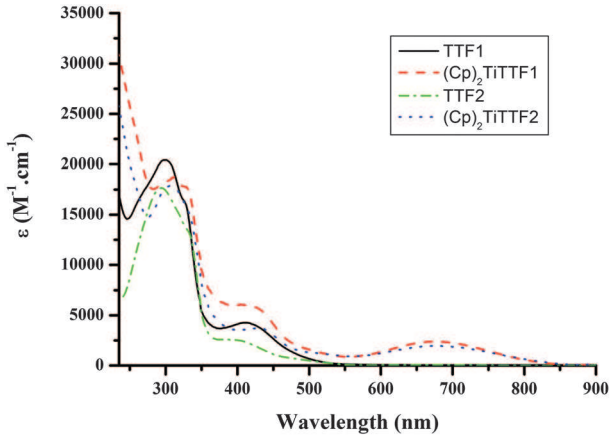

Fig. 5 Absorption spectra of **TTF1**, **TTF2**, **$(Cp)_2$Ti(TTF1)** and **$(Cp)_2$Ti(TTF2)** in dichloromethane at room temperature ($c \sim 10^{-5}$ mol L^{-1}).

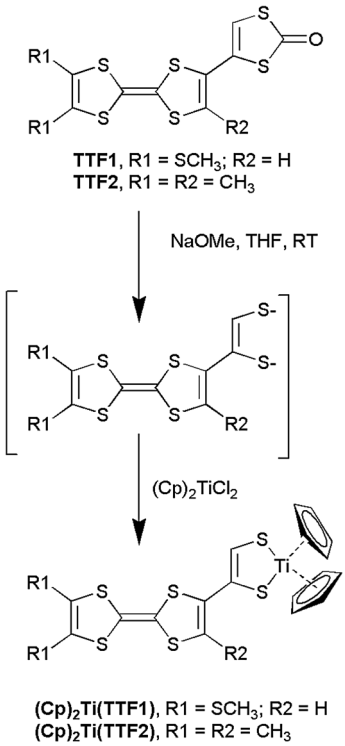

$(Cp)_2$Ti(TTF1), R1 = SCH_3; R2 = H
$(Cp)_2$Ti(TTF2), R1 = R2 = CH_3

Scheme 3 Synthetic route for the preparation of the titanium complexes.

The by-product isolated during the synthesis of **TTF2** displays a strong absorption band centred at 292 nm with a molar extinction coefficient which is almost twice that of **TTF2**. This increase in the absorption properties and the broadening of the band are attributed to the underlying absorption of the half-TTF and thiophene fragments present on the molecule. The CV displays two reversible one-electron waves at 0.32 and 0.83 V associated with the oxidation of the TTF fragment with methyl substituents to radical cations and dications respectively. An additional reversible one-electron oxidation step is also observed at 1.18 V and is attributed to the oxidation of the thiophene fragment.

Preparation and properties of dithiolene complexes

As mentioned above, the 1,3-dithiole-2-one heterocycles are excellent precursors of 1,2-dithiolate ligands, upon reaction with alkoxides. Their reaction with organometallic complexes such as $(Cp)_2TiCl_2$ is expected to provide neutral complexes, readily purified by chromatography. For this reason, the ability of our TTF-dithiolone molecules **TTF1** and **TTF2** to generate redox-active dithiolene ligands was tested here followed by their reaction with $(Cp)_2TiCl_2$ (Scheme 3). Opening of the dithiolone fragment on **TTF1** and **TTF2** was performed in the presence of 2.4 eq. of sodium methanolate. The generated dithiolate reacts *in situ* with $(Cp)_2TiCl_2$ dissolved in THF. The solution immediately turned green-brown revealing the complex formation. The targeted products, **$(Cp)_2$Ti(TTF1)** and **$(Cp)_2$Ti(TTF2)**, were easily purified by chromatography, and were isolated as green powders in moderate yields.

NMR investigation and mass spectrometry confirmed the formation of mononuclear titanium complexes carrying one pendant TTF fragment. The proton signal of the dithiolene fragment appears at a down-shielded value (7.46–7.47 ppm), compared with that observed in the dithiolone fragment (6.67 ppm). At room temperature, the proton signal of the cyclopentadienyl fragment appears as a broad peak at around 5.96–5.97 ppm. Variable-temperature ^1H NMR experiments show that this broad signal for the Cp rings splits into two sharp singlets of equal intensity at low temperature (Fig. 6). Such behaviour related to the inversion process between the two C_s conformations through the C_{2v} conformation

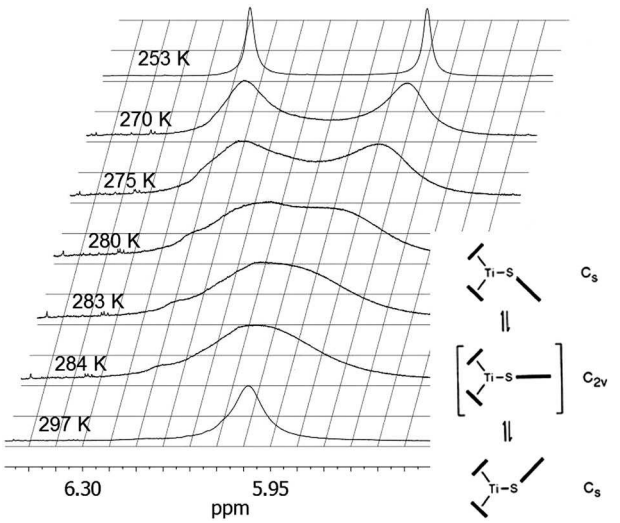

Fig. 6 Variable-temperature ^{1}H NMR spectra of **(Cp)$_2$Ti(TTF2)** in $CDCl_3$.

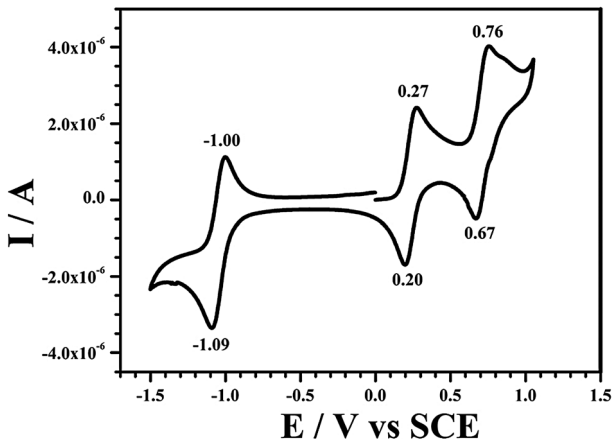

Fig. 7 Cyclic voltammogram at 0.1 V s^{-1} of the **(Cp)$_2$Ti(TTF2)** complex in CH_2Cl_2–[NBu_4][PF_6] 0.2 M at 298 K (v = 100 mV s^{-1}).

of the folded dithiolene fragment is characteristic of $(Cp)_2Ti$–dithiolene complexes (Fig. 6).[21–23] The strong folding observed in these d^0 $(Cp)_2Ti$(dithiolene) complexes finds its origin in the overlap interaction between the frontier orbitals of the $(Cp)_2Ti$ and dithiolene fragments. Indeed, in the C_{2v} unfolded symmetry, the LUMO, a_1 symmetry, a fragment orbital of the $(Cp)_2Ti$ fragment is orthogonal to the π-type HOMO of the dithiolene fragment. Folding allows for orbital mixing and is associated with a strong ligand-to-metal charge transfer. The Cp signal's coalescence is observed here at 284.5 K for **(Cp)$_2$Ti(TTF1)** and 283.5 K for **(Cp)$_2$Ti(TTF2)**, giving an activation energy ΔG of 55.7 and 55.9 kJ mol^{-1}, respectively.[24] Based on all $(Cp)_2Ti$-(dithiolene) complexes reported in ref. 9, a comparison of the activation energy of this inversion process with the actual folding angle θ – available from X-ray diffraction studies – shows that a linear correlation can be established, which reads in chlorinated solvents as: $\theta = 0.28 \times \Delta G + 31$ (ΔG in kJ mol^{-1} and θ in °). From this equation, and in the absence of X-ray crystal structure for our complexes, the folding angles for **(Cp)$_2$Ti(TTF1)** and **(Cp)$_2$Ti(TTF2)** can be estimated to amount to $\approx 47°$ for both complexes.[21–23]

The slight red-shift of the UV absorption bands associated with $^1\pi$–π^* transitions localized on the TTF cores is attributed to the donating effect of the dithiolene fragment (Fig. 5). The strong increase in the absorption below 280 nm observed with the complexes is due to the presence of the cyclopentadienyl fragments. An additional band centred at 680 nm is responsible for the green color of the complex. This low-energy absorption band is attributed to an electronic transition from the HOMO (Lπ) to the LUMO (Lπ^*-αd_{xy}) with metallic character.[25]

The CV of **(Cp)$_2$Ti(TTF1)** and **(Cp)$_2$Ti(TTF2)** exhibits the same shape, *i.e.* a reversible one-electron reduction wave, attributable to the metal-centred $Ti^{(IV)} \rightarrow Ti^{(III)}$ process and two reversible one-electron oxidation waves attributed to the formation of the TTF radical cation and dication, respectively (Fig. 7). Remarkably, the TTF cores are more easily oxidized in their cyclopentadienyl–dithiolene titanium complexes, compared with the parent molecules, due to the electron donating ability of the electron rich dithiolene ligand. The titanium centre is also more difficult to reduce due to the presence of the electron rich TTF moiety and the reduction wave is cathodically shifted by *ca.* 0.3 V, when compared with the reduction of $(Cp)_2TiCl_2$.

Conclusions

In the present work, the synthesis of TTF molecules appended with one 1,3-dithiol-2-one moiety was undertaken in order to test their ability after ring opening to form stable metal–dithiolene complexes. **TTF1** was synthesized using the phosphite-mediated cross-coupling method. However, the overall reaction yield hardly exceeded 30% and large quantities of **TMT-bi-TTF** were also isolated. For this reason, an original radical synthetic route using diisopropylxanthogen disulfide was explored to directly convert the alkynyl function of an ethynyltrimethyl-TTF molecule into 1,3-dithiol-2-one. Reaction yields around 60% have been reached for the preparation of **TTF2** and an intriguing by-product has also been isolated and fully characterized. These TTF molecules appended with one 1,3-dithiol-2-one moiety can efficiently be opened with a base to lead to the formation of TTF functionalized dithiolene ligands. Their complexation ability toward metal ions was validated using the $(Cp)_2TiCl_2$ precursor. Two original titanium green complexes have been isolated and characterized. The inversion process, characteristic of cyclopentadienyl–dithiolene complexes, has been studied by temperature-dependent NMR experiments and from the extracted activation energies a folding angle around 47° has been estimated. The preparation of dithiolone fragments from alkyne groups is an attractive synthetic route which allows for the preparation of a wide variety of functional dithiolene ligands. In the next step, it will now be interesting to isolate metal–bis(dithiolene) complexes with the functional TTF described here for the synthesis of new single component metallic materials. Work along these lines is currently in progress in our laboratory.

We are also trying to get some molecular conductors with these newly prepared TTF containing titanocene complexes by electrocrystallization.

Experimental section

General

300 (^{1}H) and 75.5 MHz (^{13}C) NMR spectra were recorded on a Bruker Avance 300 spectrometer at room temperature using perdeuterated solvents. Variable-temperature ^{1}H NMR studies were performed on a Bruker Avance 400III spectrometer. Chemical shifts are reported in ppm referenced to TMS for ^{1}H NMR and ^{13}C NMR. FT-IR spectra were recorded using a Varian-640 FT-IR spectrometer equipped with a PIKE ATR apparatus. High resolution mass spectra were recorded using a Varian MAT 311 instrument by the Centre Régional de Mesures Physiques de l'Ouest, Rennes. Elemental analyses were performed at the Centre Régional de Mesures Physiques de l'Ouest, Rennes, and the Service de microanalyse of the ICSN at Gif-sur-Yvette. UV-Vis spectra were recorded on a Cary 100 scan UV-Vis spectrophotometer (Varian, Australia). Samples were placed in 1 cm path length quartz cuvettes. Cyclic voltammetry measurements were performed using an Autolab electrochemical analyzer (PGSTAT 30 potentiostat/galvanostat from Eco Chemie B.V.) equipped with the GPES software in a three-electrode glass cell. The working electrode was a 1 mm diameter platinum disk and the counter electrode was a glassy carbon rod. All reported potentials are referred to a KCl Saturated Calomel Electrode (SCE) (uncertainty ±5 mV). Tetra-*n*-butylammonium hexafluorophosphate Bu_4NPF_6 was purchased from Fluka (puriss, electrochemical grade) and was used, as received, at 0.2 mol L^{-1} as a supporting electrolyte in anhydrous methylene chloride. All electrochemical measurements were carried out inside a Faraday cage, at room temperature (20 ± 2 °C) and under constant argon flow. The resistance of the electrolytic cell was compensated by positive feedback.

Syntheses

Anhydrous CH_2Cl_2 and THF were obtained by distillation over P_2O_5 and Na/benzophenone respectively. Triethylphosphite was freshly distilled prior to use. All synthetic manipulations were performed under an inert and dry nitrogen atmosphere. All other reagents and materials from commercial sources were used without further purification. Silica gel used in chromatographic separations was obtained from Acros Organics (Silica Gel, ultra pure, 40–60 μm). 4,4′-Bis(1,3-dithiole-2-one),[26] 4,5-bis(methylthio)-1,3-dithiole-2-one[27] and ethynyltrimethyl-TTF ($HC{\equiv}CMe_3TTF$)[16,17] were prepared according to the previously published procedure.

Diisopropylxanthogen disulfide was prepared using a method derived from that of Pound, Klumperman *et al.*[28] Potassium isopropylxanthate (3 g, 17.2 mmol) was dissolved in distilled water (30 mL). A solution of iodine (0.99 g, 3.9 mmol) and potassium iodide (0.51 g, 3.1 mmol) in distilled water (90 mL) was added dropwise and the solution was stirred after complete addition for 24 h. The product was extracted from the aqueous solution with dichloromethane. The organic phase was dried over $MgSO_4$ and evaporation of the solvent allowed the isolation of the diisopropylxanthogen disulfide as a light yellow oil (0.93 g, 3.4 mmol) (yield = 40%). ^{1}H NMR ($CDCl_3$, 300 MHz) δ (ppm) 5.66 (heptuplet, ^3J = 6.1 Hz, 2H, CH), 1.38 (doublet, ^3J = 6.3 Hz, 12H, CH_3).

Synthesis of TTF1

4,4′-Bis(1,3-dithiole-2-one) (100 mg, 0.43 mmol) and 4,5-bis-(methylthio)-1,3-dithiole-2-one (65 mg, 0.29 mmol) were dissolved in 10 mL of freshly distilled $P(OEt)_3$. The solution was stirred at 110 °C under N_2 for 1 h. The solvent was evaporated to give crude products which were chromatographed on silica gel with CS_2/CH_2Cl_2 (100/0 to 90/10% v/v) to afford **TTF1** (37 mg, yield = 31%) as an orange powder, together with **TMT-bi-TTF** (19 mg, yield = 13%). The products were dissolved in a 1 : 1 CH_2Cl_2 : MeOH solvent mixture and crystallized by slow evaporation.

TTF1

^{1}H NMR ($CDCl_3$, 300 MHz) δ 2.43 (s, 6H, SCH_3), 6.35 (s, 1H, CH), 6.55 (s, 1H, CH); ^{13}C NMR ($CDCl_3$, 75.5 MHz) 19.4 (CH_3), 110.8, 111.5, 115.3, 119.0, 126.1, 127.5, 127.6, 127.9, 190.2 (C═O); UV-vis (CH_2Cl_2, 20 °C): λ_{max} (ε, M^{-1} cm^{-1}) = 300 (20 500), 328 (16 000), 410 (4300); IR (ATR, cm^{-1}): 2964, 2919, 1641(νC═O), 1557, 1429, 1275, 1261, 1205, 1093, 1020, 968, 882, 845, 803, 764, 750, 730, 670, 649; anal. calcd for $C_{11}H_8OS_8$: C, 32.01; H, 1.95; S, 62.16; found C, 32.73; H, 2.02%; HRMS (ESI/ASAP Q-tof 2): m/z (%) = 412.8410 (2 ppm) $[M + H]^+$.

TMT-bi-TTF

^{1}H NMR ($CDCl_3$, 300 MHz) δ 2.42 (s, 12H, SCH_3), 6.22 (s, 2H, CH); ^{13}C NMR ($CDCl_3$, 75.5 MHz) 19.38 (CH_3), 110.4, 112.2, 118.7, 126.9, 127.6, 127.7, 127.8; UV-vis (CH_2Cl_2, 20 °C): λ_{max} (ε, M^{-1} cm^{-1}) = 263 (22 000), 314 (24 000), 327 (24 000), 406 (7400); IR (ATR, cm^{-1}): 2922, 2853, 1458, 1425, 1376, 1366, 1305, 1261, 1228, 1192, 1086, 1020, 955, 893, 844, 777, 747, 712, 669, 652, 635; anal. calcd for $C_{16}H_{14}S_{12}$: C, 32.51; H, 2.39; S, 65.10; found C, 32.51; H, 2.31; S, 65.46%; HRMS (ESI/ASAP Q-tof 2): m/z (%) = 589.7742 (0 ppm) $[M^{+\bullet}]$.

Synthesis of TTF2

Ethynyltrimethyl-TTF (150 mg, 0.56 mmol) was dissolved in 5.6 mL of a 0.1 M solution of diisopropylxanthogen disulfide in benzene (0.56 mmol) in a Schlenk tube under nitrogen. AIBN (42 mg, 0.45 eq., 0.25 mmol) was added and the solution was stirred at 80 °C for 48 h. After evaporation of the solvent, the product was purified by column chromatography on silica gel pretreated with 10% triethylamine using a 15/85% v/v CH_2Cl_2–petroleum ether solvent mixture. The product was isolated as an orange powder in good yield (120 mg, 60%), together with another orange by-product (65 mg, 27%). The products were dissolved in a 1 : 1 CH_2Cl_2 : MeOH solvent mixture and crystallized by slow evaporation.

TTF2

^{1}H NMR ($CDCl_3$, 300 MHz) δ 1.95 (s, 6H, CH_3), 2.13 (s, 3H, CH_3), 6.67 (s, 1H, CH); $^{13}C\{^1H\}$ DEPT NMR ($CDCl_3$, 75.5 MHz) 13.9 (CH_3), 15.5 (CH_3), 104.2 (C_q), 112.7 (C_q), 117.8 (CH), 119.1 (C_q), 123.0 (C_q), 123.1 (C_q), 125.3 (C_q), 131.8 (C_q), 191.6 (C═O); UV-vis (CH_2Cl_2, 20 °C): λ_{max} (ε, M^{-1} cm^{-1}) = 294 (17 700), 334 (13 000), 394 (2500); IR (ATR, cm^{-1}): 3047, 2992, 2909, 2845, 1630 (νC═O), 1591, 1435, 1275, 1260, 1235, 1182, 1119, 1091, 1028, 881, 821, 777, 749, 719, 668, 647, 628; anal. calcd for $C_{12}H_{10}OS_6$: C, 39.75; H, 2.78; S, 53.06; found C, 39.71; H, 2.88; S, 53.24%; HRMS (ESI/ASAP Q-tof 2): *m*/*z* (%) = 362.9134 (0 ppm) $[M + H]^+$.

By-product

^{1}H NMR ($CDCl_3$, 300 MHz) δ 1.33 (m, 12H, CH_3), 1.92 (m, 12H, CH_3), 1.97 (s, 3H, CH_3), 5.69 (m, 2H, *CH*(CH_3)$_2$), 6.38 (s, 1H, CH), 7.44 (s, 1H, CH); $^{13}C\{^1H\}$ DEPT NMR ($CDCl_3$, 75.5 MHz) 13.6 (CH_3), 13.85 (CH_3), 13.9 (CH_3), 16.1 (CH_3), 16.5 (CH_3), 21.3 (CH_3), 21.4 (CH_3), 78.4 (CH), 78.6 (CH), 98.4 (C_q), 107.0 (C_q), 109.2 (C_q), 117.8 (C_q), 122.7 (C_q), 123.1 (C_q), 123.4 (C_q), 124.9 (C_q), 125.7 (C_q), 128.7 (C_q), 130.0 (CH), 130.2 (C_q), 131.1 (C_q), 142.5 (CH), 146.4 (C_q), 157.0 (C_q), 210.7 (C_q), 212.2 (C_q); UV-vis (CH_2Cl_2, 20 °C): λ_{max} (ε, M^{-1} cm^{-1}) = 292 (36 500), 334 (27 000), 365 (14 000), 472 (1000); IR (ATR, cm^{-1}): 3005, 2987, 1541, 1488, 1434, 1372, 1338, 1275, 1253, 1086, 1024, 901, 860, 798, 764, 750, 668, 649, 616; anal. calcd for $C_{30}H_{34}O_2S_{13}$: C, 42.72; H, 4.06; S, 49.42; found C, 42.63; H, 4.11; S, 49.64%; HRMS calc. for (ESI MicrO-Tof-Q II): *m*/*z* (%) = 841.8921 (0 ppm) $[M^{+\bullet}]$.

General procedure for the preparation of cyclopentadienyl–dithiolene titanium complexes

TTF1 or **TTF2** (40 mg) was dissolved in 10 mL of dry THF under nitrogen in a Schlenk tube and 2.4 eq. of sodium methanolate (1 M in methanol) were injected dropwise into the solution under stirring. After complete addition, the solution was stirred at room temperature for 1 hour and then 1.1 eq. of bis(cyclopentadienyl)titanium dichloride dissolved in 5 mL of dry THF were injected into the solution under stirring. After addition the solution immediately turned green-brown and the solution was left under stirring for 3 h. After removal of the solvent, the product was directly purified by column chromatography on silica gel using a 75/25 (%v/v) CS_2–CH_2Cl_2 mixture as an eluent. After evaporation of the eluent, the product was reprecipitated as a green powder from a 1 : 1 CH_2Cl_2 : MeOH solvent mixture after slow evaporation of the methanol.

$(Cp)_2Ti$(TTF1)

Green powder, 13.2 mg (24%), ^{1}H NMR ($CDCl_3$, 300 MHz) δ 2.42 (s, 3H, SCH_3), 2.43 (s, 3H, SCH_3), 5.96 (br, 10H, H(Cp), 6.53 (s, 1H, CH), 7.46 (s, 1H, CH). ^{13}C NMR ($CDCl_3$, 75.5 MHz) 19.37 (CH_3), 107.41, 111.00 (broad peak C(Cp)), 112.1, 113.1, 115.7, 117.5, 127.4, 127.9, 136.9, 147.7, 149.0; UV-vis (CH_2Cl_2, 20 °C): λ_{max} (ε, M^{-1} cm^{-1}) = 298 (18 300), 312 (18 700), 329 (17 700), 415 (6000), 673 (2400); IR (ATR, cm^{-1}): 2959, 2920, 2850, 1740, 1457, 1430, 1260, 1091, 1017, 884, 813, 755, 730, 704, 632; HRMS for $C_{20}H_{18}S_8Ti$ (ESI MicrO-Tof-Q II): *m*/*z* (%) = 561.8650 (0 ppm) $[M^{+\bullet}]$.

$(Cp)_2Ti$(TTF2)

Green powder, 17.2 mg (30%), ^{1}H NMR ($CDCl_3$, 300 MHz) δ 1.93 (s, 6H, CH_3), 2.21 (s, 3H, CH_3), 5.97 (br, 10H, H(Cp)), 7.47 (s, 1H, CH). $^{13}C\{^1H\}$ DEPT NMR ($CDCl_3$, 75.5 MHz) 13.9 (CH_3), 15.8 (CH_3), 110.6 (broad peak C(Cp)), 122.8 (C_q), 123.1 (C_q), 125.5 (C_q), 131.1 (C_q), 149.0 (CH), 150.2 (C_q); UV-vis (CH_2Cl_2, 20 °C): λ_{max} (ε, M^{-1} cm^{-1}) = 307 (18 000), 332 (15 000), 430 (3700), 680 (1900); IR (ATR, cm^{-1}): 2960, 2923, 2852, 1733, 1457, 1436, 1375, 1260, 1089, 1017, 800, 740, 705, 631; HRMS for $C_{21}H_{20}S_6Ti$ (ESI MicrO-Tof-Q II): *m*/*z* (%) = 511.9365 (0 ppm) $[M^{+\bullet}]$.

X-Ray crystallography

X-ray crystal structure determinations were performed on an APEXII Bruker-AXS diffractometer equipped with a CCD camera and a graphite-monochromated MoKα radiation source (λ = 0.71073 Å), from the Centre de Diffractométrie (CDFIX), Université de Rennes 1, France. Structures were solved by direct methods using the *SIR97* program,[29] and then refined with full-matrix least-square methods based on F^2 (*SHELXL-97*)[30] with the aid of the *WINGX* program.[31] For complexes **2** and **3**, the contribution of the disordered solvents to the calculated structure factors was estimated following the *BYPASS* algorithm,[32] implemented as the *SQUEEZE* option in *PLATON*.[33] A new data set, free of solvent contribution, was then used in the final refinement. All non-hydrogen atoms were refined with anisotropic atomic displacement parameters. H atoms were finally included in their calculated positions.

Crystal structure determination of TTF1 at 150 K

Crystal data. Red prism, $C_{11}H_8OS_8$, M = 412.65, triclinic, a = 10.1011(17) Å, b = 11.4452(18) Å, c = 15.124(2) Å, α = 69.997(7)°, β = 81.790(7)°, γ = 73.284(7)°, V = 1571.6(4) Å^3, T = 150(2) K, space group $P\bar{1}$, Z = 4, μ(MoKα) 0.71073 Å, 21 733 reflections measured, 7130 independent reflections (R_{int} = 0.0457) of which 5858 reflections with $I > 2\sigma(I)$ were used for the refinement of 361 parameters. The final R and w$R(F)$ are 0.0336 and 0.0875, respectively.

Crystal structure determination of TMT-bi-TTF at 150 K

Crystal data. Red plate, $C_{16}H_{14}S_{12}$, M = 591.11, orthorhombic, a = 15.341(3) Å, b = 29.058(6) Å, c = 5.1928(10) Å, V = 2314.9(8) Å^3, T = 150(2) K, space group $Pn2_1a$ (non-standard setting of space group $Pna2_1$), Z = 4, μ(MoKα) 0.71073 Å, 36 533 reflections measured, 5302 independent reflections (R_{int} = 0.0891) of which 4082 reflections with $I > 2\sigma(I)$ were used for the refinement of 257 parameters. The Flack parameter for this configuration is 0.5(2). The overall quality of the dataset is relatively poor, leading to spurious peaks and holes of residual electron density. The final R and w$R(F)$ are 0.0646 and 0.1468, respectively.

Crystal structure determination of TTF2 at 293 K

Crystal data. Orange prism, $C_{12}H_{10}OS_6$, M = 362.56, monoclinic, a = 14.1392(2) Å, b = 6.92050(10) Å, c = 30.6289(5) Å,

β = 94.1250(10)°, V = 2989.28(8) Å^3, T = 293(2) K, space group $C2/c$, Z = 8, μ(MoKα) 0.71073 Å, 21 314 reflections measured, 3413 independent reflections (R_{int} = 0.0483) of which 2835 reflections with $I > 2\sigma(I)$ were used for the refinement of 172 parameters. The final R and w$R(F)$ are 0.0369 and 0.0843, respectively.

Crystal structure determination of the by-product at 293 K

Crystal data. Orange sword, $C_{30}H_{34}O_2S_{13}$, M = 843.35, triclinic, a = 7.569(5) Å, b = 14.725(5) Å, c = 18.158(5) Å, α = 95.476(5)°, β = 90.546(5)°, γ = 91.274(5)°, V = 2013.9(16) Å^3, T = 293(2) K, space group $P\bar{1}$, Z = 2, μ(MoKα) 0.71073 Å, 29 876 reflections measured, 9193 independent reflections (R_{int} = 0.1813) of which 3954 reflections with $I > 2\sigma(I)$ were used for the refinement of 416 parameters. The final R and w$R(F)$ are 0.0668 and 0.1683, respectively.

Acknowledgements

Financial support from the CNRS is gratefully acknowledged. G.Y. thanks Ministère de la Recherche for his PhD grant.

Notes and references

1 (*a*) Special issue on Molecular conductors, P. Batail, *Chem. Rev.*, 2004, **104**, 4887–5781; (*b*) G. Saito and Y. Yoshida, *Bull. Chem. Soc. Jpn.*, 2007, **80**, 1–137.

2 (*a*) R. Zahradník, P. Čársky, S. Hünig, G. Kiesslich and D. Scheuzow, *Int. J. Sulfur Chem., Part C*, 1971, **6**, 109–122; (*b*) K. Deuchert and S. Hünig, *Angew. Chem., Int. Ed. Engl.*, 1978, **17**, 875–886 and references therein; (*c*) S. Leroy-Lhez, J. Baffreau, L. Perrin, E. Levillain, M. Allain, M.-J. Blesa and P. Hudhomme, *J. Org. Chem.*, 2005, **70**, 6313–6320; (*d*) I. A. Latif, V. P. Singh, U. Bhattacharjee, A. Panda and S. N. Datta, *J. Phys. Chem. A*, 2010, **114**, 6648–6656.

3 D. Canevet, M. Sallé, G. Zhang, D. Zhang and D. Zhu, *Chem. Commun.*, 2009, 2245–2269.

4 (*a*) D. Lorcy, N. Bellec, M. Fourmigué and N. Avarvari, *Coord. Chem. Rev.*, 2009, **253**, 1398–1438; (*b*) M. Shatruk and L. Ray, *Dalton Trans.*, 2010, **39**, 11105–11121; (*c*) J. Massue, N. Bellec, S. Chopin, E. Levillain, T. Roisnel, R. Clérac and D. Lorcy, *Inorg. Chem.*, 2005, **44**, 8740–8748; (*d*) N. Bellec, J. Massue, T. Roisnel and D. Lorcy, *Inorg. Chem. Commun.*, 2007, **10**, 1172–1176.

5 H. Tanaka, Y. Okano, H. Kobayashi, W. Suzuki and A. Kobayashi, *Science*, 2001, **291**, 285.

6 (*a*) K. Saito, M. Nakano, H. Tamura and G.-E. Matsubayashi, *Inorg. Chem.*, 2000, **39**, 4815–4820; (*b*) K. Saito, M. Nakano, H. Tamura and G.-E. Matsubayashi, *J. Organomet. Chem.*, 2001, **625**, 7–12; (*c*) G.-E. Matsubayashi, M. Nakano, K. Saito and H. Tamura, *Mol. Cryst. Liq. Cryst.*, 2000, **343**, 29–34; (*d*) R. D. McCullough, J. A. Belot, J. Seth, A. L. Rheingold, G. P. A. Yap and D. O. Cowan, *J. Mater. Chem.*, 1995, **5**, 1581–1587; (*e*) R. D. McCullough, J. A. Belot, A. L. Rheingold and G. P. A. Yap, *J. Am. Chem. Soc.*, 1995, **117**, 9913–9914; (*f*) R. D. McCullough and J. A. Belot, *Chem. Mater.*, 1994, **6**, 1396–1403.

7 See also: S.-K. Lee, K.-S. Shin, D.-Y. Noh, O. Jeannin, F. Barrière, J.-F. Bergamini and M. Fourmigué, *Chem.–Asian J.*, 2010, **5**, 169–176.

8 B. Garreau-de Bonneval, K. I. Moineau-Chane Ching, F. Alary, T.-T. Bui and L. Valade, *Coord. Chem. Rev.*, 2010, **254**, 1457–1467.

9 M. Fourmigué, *Coord. Chem. Rev.*, 1998, **178–180**, 823–864.

10 K. Sato, M. Kusakabe, T. Watanabe and H. Tatemitsu, *Synth. Met.*, 1995, 1949–1950.

11 D. E. John, A. J. Moore, M. R. Bryce, A. S. Batsanov, M. A. Leech and J. A. K. Howard, *J. Mater. Chem.*, 2000, **10**, 1273–1279.

12 M. Iyoda, K. Hara, E. Ogura, T. Takano, M. Hasegawa, M. Yoshida, Y. Kuwatani, H. Nishikawa, K. Kikuchi, I. Ikemoto and T. Mori, *J. Solid State Chem.*, 2002, **168**, 597–607.

13 Y. Gareau and A. Beauchemin, *Heterocycles*, 1998, **48**, 2003–2017.

14 (*a*) S. Dalgleish and N. Robertson, *Chem. Commun.*, 2009, 5826–5828; (*b*) S. Dalgleish, K. Awaga and N. Robertson, *Chem. Commun.*, 2011, **47**, 7089–7091.

15 (*a*) T. Otsubo, Y. Kochi, A. Bitoh and F. Ogura, *Chem. Lett.*, 1994, 2047–2050; (*b*) C. Goze, S.-X. Liu, C. Leiggener, L. Sanguinet, E. Levillain, A. Hauser and S. Decurtins, *Tetrahedron*, 2008, **64**, 1345–1350; (*c*) A. S. Andersson, L. Kerndrup, A. O. Madsen, K. Kilsa, M. Brondsted Nielsen, P. R. La Porta and I. Biaggio, *J. Org. Chem.*, 2009, **74**, 375–382; (*d*) D. Cao, C. Wang, M. A. Giesener, Z. Liu and J. F. Stoddart, *Chem. Commun.*, 2012, **48**, 6791–6793.

16 A. Vacher, F. Barriere, T. Roisnel and D. Lorcy, *Chem. Commun.*, 2009, 7200–7202.

17 A. Vacher, F. Barriere, T. Roisnel, L. Piekara-Sady and D. Lorcy, *Organometallics*, 2011, **30**, 3570–3578.

18 A. Miyazaki, Y. Ogyu, F. Justaud, L. Ouahab, T. Cauchy, J.-F. Halet and C. Lapinte, *Organometallics*, 2010, **29**, 4628–4638.

19 A. Vacher, F. Barriere, F. Camerel, J.-F. Bergamini, T. Roisnel and D. Lorcy, *Dalton Trans.*, 2013, **42**, 383–394.

20 G. Yzambart, B. Fabre and D. Lorcy, *Langmuir*, 2012, **28**, 3453–3459.

21 F. Guyon, C. Lenoir, M. Fourmigué, J. Larsen and J. Amaudrut, *Bull. Soc. Chim. Fr.*, 1994, **131**, 217–226.

22 S. Zeltner, W. Dietzsch, R.-M. Olk, R. Kirmse, R. Richter, U. Shröder, B. Olk and E. Hoyer, *Z. Anorg. Allg. Chem.*, 1994, **620**, 1768–1776.

23 S. Eid, T. Roisnel and D. Lorcy, *J. Organomet. Chem.*, 2008, **693**, 2755–2760.

24 H. Eyring, *Chem. Rev.*, 1935, **17**, 65.

25 K. Ohta, H. Hasebe, H. Ema, M. Moriya, T. Fujimoto and I. Yamamoto, *Mol. Cryst. Liq. Cryst.*, 1991, **208**, 21–32.

26 J. R. Andersen, V. V. Patel and E. M. Engler, *Tetrahedron Lett.*, 1978, **19**, 239–242.

27 N. Svenstrup and J. Becher, *Synthesis*, 1995, 215–235 and references therein.
28 G. Pound, J. M. McKenzie, R. F. M. Lange and B. Klumperman, *Chem. Commun.*, 2008, 3193–3195.
29 A. Altomare, M. C. Burla, M. Camalli, G. Cascarano, C. Giacovazzo, A. Guagliardi, A. G. G. Moliterni, G. Polidori and R. Spagna, *J. Appl. Crystallogr.*, 1999, **32**, 115–119.
30 G. M. Sheldrick, *Acta Crystallogr., Sect. A: Fundam. Crystallogr.*, 2008, **64**, 112–122.
31 L. J. J. Farrugia, *J. Appl. Crystallogr.*, 1999, **32**, 837–838.
32 P. van der Sluis and A. L. Spek, *Acta Crystallogr., Sect. A: Fundam. Crystallogr.*, 1990, **46**, 194–201.
33 A. L. Spek, *Acta Crystallogr., Sect. D: Biol. Crystallogr.*, 2009, **65**, 148–155.